Impedance Dependency on Planar Broadband Dipole Dimensions: An Examination with Antenna Equivalent Circuits

Tommi Tuovinen* and Markus Berg

Abstract—The present paper considers the connection between complex input impedance and the physical dimensions for planar ultra wideband (UWB) antennas. The first time the effect of both the actual radiator width and length for impedance behaviour is comprehensively presented. Also the effect of feed point dimensions on complex impedance is studied. The investigations involve both UWB single-resonant dipoles to cover bandwidth $\geq 500\,\text{MHz}$ and a multi-resonant dipole for the entire Federal Communications Commission's (FCC) frequency band of 3.1–10.6 GHz. Lumped-element equivalent circuits are used identically with 3D antenna simulations in order to observe the corresponding impedance behaviour with the studied antennas. The used equivalent circuits consisting of series- and parallel-resonant stages are widely accepted in the open literature. The series-resonant circuit of equivalent is observed to have the analogue to the antenna feeding area. The physical dipole dimensions in terms of a length and width are connected to parallel-resonant part, which mainly determines the antenna input impedance. The resistance of a parallel-resonant stage behaves as the maximum value of real part of dipole impedance with an influence on bandwidth together with the ratio of parallel capacitance C and inductance L. The increase of the antenna physical width has an effect on bandwidth, because of the wider the antenna, the higher the capacitance in the antenna feed. Since the traditional dipoles are used for these studies, the results can be extended in several ways for other antenna types or, for instance, to verify the effect of body tissue, close to a wearable antenna.

1. INTRODUCTION

Ultra wideband (UWB) [1, 2] technology has sparked intense interest during the last decade. Low complexity and spectral power density, resulting in small interference to existing systems, makes the UWB an attractive approach, e.g., for a future short-range high-data transfer wireless communications. Due to the wide response of UWB (from 3.1 to 10.6 GHz), defined by Federal Communications Commission (FCC) [1], the antenna structures have become complicated, because of the need for multiple resonances to cover the large bandwidth (BW), which is not achieved with a single-resonant antenna. Also the impulse kind of nature of UWB increases the challenge of antenna design since the reflection coefficient S_{11} should appear as non-resonant type (i.e., smooth) to diminish the harmful ringing effect [2] that might be strong for antennas having high impedance variation over the frequency band. Challenges of the co-design of UWB antenna/circuit interface are also reported in [3, 4]. Since matching circuits can cause additional time-delays [5] for a broadband antenna and typically increase transmission loss, the impedance matching components for UWB are not feasible in practice. Recently, several UWB antennas have been reported for various purpose of use, e.g., in [6–12].

Lumped-element equivalent circuits have been customary for characterizing properties for the antenna input impedance Z_{in}. Equivalents can be applied in many ways as, for instance, 1) to model an

* Corresponding author: Tommi Tuovinen (tommi.tuovinen@ee.oulu.fi).

The authors are with the Department of Communications Engineering, Centre for Wireless Communications, University of Oulu, P. O. Box 4500, Oulu 90014, Finland.

antenna, 2) to understand the antenna operation, 3) to compute the antenna matching potential [13], and so forth. Naturally, the impedance properties of a circuit model must correlate perfectly with the modelled antenna [14], which might cause challenge especially for UWB antennas since the parameters are frequency-dependent [3]. Since UWB antennas are characterized to act as a pulse-shaping filter [2], it is proposed that equivalent model should also be to capture a possible UWB antenna waveform distortion [15] in order that a designer can find out ways to mitigate it.

Various extensive studies have been reported regarding the antenna equivalent circuits, e.g., in [16–19] for dipoles. It is observed that the proposed models are able to present antenna impedance properties, but only in terms of input impedance. However, it is challenging to find an article where reflection coefficient S_{11} results are also depicted by an equivalent circuit for a wideband antenna, even though S_{11} is the parameter that antenna designer should first to qualify of antenna system requirements. Further, it is surprising that the analogue between the equivalents and broadband antennas has not so far presented in detail for UWB radiators. The purpose of the present paper is to examine an impedance dependency on wideband dipole dimensions, and to demonstrate the effect of changing the component values of the equivalent circuit in comparison with the physical dimensions of simulated dipoles.

This paper is organized as follows. First, planar UWB dipole antenna simulation models that are redesigns of the traditional single- and multi-resonant dipole structures are designed for the frequencies of interest. Then, antenna equivalent circuit model structures to be studied are chosen based on the literature review in the previous publications [3, 16, 18] and common circuit theory [20]. Finally, the circuit component values are defined by following the consideration of the correspondence between equivalents and physical antenna dimensions.

All simulations (including time domain transients for antennas and circuit verification for equivalent models) are carried out with Computer Simulation Technology (CST) Microwave Studio [21], which is widely used both in industry and academic.

2. BROADBAND DIPOLE ANTENNAS AND LUMPED-ELEMENT EQUIVALENT CIRCUITS

It is observed that various types of antennas are designed and used for UWB in the open literature. The dipole was chosen to be the antenna to study, since the operation of most of the antenna types can be explained based on a dipole. For this reason the information in this paper can be further applied for other antennas. On the other hand, many studies have been reported where a conventional dipole (or monopole) is used for the wide range of applications [6–10, 16–18, 25] because of its feasible characteristics such as omnidirectional radiation, the smooth gain of roughly 2 dBi, easy to tune and low cost to fabricate.

2.1. Planar Single- and Multi-Resonant Ultra Wideband Dipoles

Three single-resonant dipole antennas are designed for the centre frequencies f_c of 3 GHz, 6 GHz and 9 GHz. The studied antennas consist of two printed metallic strips with a length L_D and W_D, and a feed gap F_D in between them. Fractional bandwidth of $f_B = (f_{\text{high}} - f_{\text{low}})/f_{\text{centre}}$ for $|S_{11}| \leq -10$ dB of the dipoles is determined to be $f_B = 0.5$, 1 and 1.5 for 3 GHz, 6 GHz and 9 GHz, respectively. A 1.57 mm thickFR4 substrate with the dielectric constant $\varepsilon_r = 4.3$ is used below the radiator. The area of substrate is extended over the edges of radiators in order to slightly compensate the body effect in terms of detuning. Because of the substrate, the lengths of half-wave antennas are 0.31λ (3 GHz), 0.33λ (6 GHz) and 0.34λ (9 GHz) in comparison with the free space wavelength.

A multi-resonant dipole, which covers the entire FCC UWB band of 3.1–10.6 GHz, is shown in Figure 1. Two extremely narrow strips are added for the feed alignment of a discrete port in between the dipole plates. Wide frequency operation is achieved by extending both the width of the antenna and shaping the curvature form for the antenna pattern close to the feeding. For a practical multi-resonant UWB antenna, the shape of feeding lines, the feed gap dimensions and the way to excite the antenna have more significant effect on Z_{in} [22] in comparison with the single-resonant counterpart.

Each designed antenna exhibits linear polarization and satisfies the FCC definition [1] of 500 MHz $S_{11} \leq -10$ dB bandwidth. The fundamental dimensions for the single- and multi-resonant antennas are
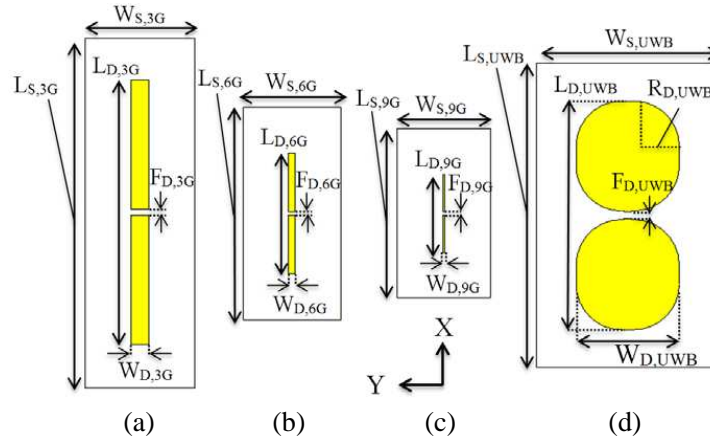
Figure 1. CST antenna simulation models for designed planar UWB dipoles: single-resonants for (a) 3 GHz, (b) 6 GHz and (c) 9 GHz, and (d) multi-resonant.

Table 1. Dimensions for the designed simulated antennas in Figure 1.

Antenna parameters	Dimensions in mm	Substrate parameters	Dimensions in mm
$L_{D,3\mathrm{G}}$	34.7	$L_{S,3\mathrm{G}}$	46.0
$L_{D,6\mathrm{G}}$	15.9	$L_{S,6\mathrm{G}}$	27.9
$L_{D,9\mathrm{G}}$	10.3	$L_{S,9\mathrm{G}}$	22.3
$L_{D,\mathrm{UWB}}$	30.1	$L_{S,\mathrm{UWB}}$	40.1
$W_{D,3\mathrm{G}}$	2.4	$W_{S,3\mathrm{G}}$	15.0
$W_{D,6\mathrm{G}}$	0.9	$W_{S,6\mathrm{G}}$	12.9
$W_{D,9\mathrm{G}}$	0.3	$W_{S,9\mathrm{G}}$	12.3
$W_{D,\mathrm{UWB}}$	13.6	$W_{S,\mathrm{UWB}}$	24.0

summarized on Table 1. Antenna feed gaps F_D of 0.7 mm (3 GHz), 0.4 mm (6 GHz), 0.4 mm (9 GHz) and 0.9 mm (UWB) are used. The radius $R_{D,\mathrm{UWB}}$ of 6 mm is used for the rounding of UWB dipole corners.

2.2. Equivalent Circuits for Single- and Multi-Resonant Dipole Antennas

Impedance of a series-resonant circuit consisting of inductance L_n and capacitance C_n is known to be minor in resonance, where the impedance maximum value for a parallel-resonant circuit is achieved. In theory, a resonance frequency f_{res} for a circuit including L_n and C_n can be given by the well-known equation [20]

$$f_{res} = \frac{1}{2\pi\sqrt{L_n C_n}}. \tag{1}$$

The chosen equivalent circuit structure for single-resonant UWB dipoles is shown in Figure 2(a). This structure is widely accepted, as can be found from many papers, e.g., in [3, 16]. In this study, the model is determined for the wideband single-resonant dipoles in Figure 1, evaluated further for the operation of multi-resonant dipole, and finally applied for the characterization of their impedance behaviour.

The equivalent consists of the series- and parallel-resonant circuits. The determination of circuit values is empirical-based, since equivalents are evaluated based on the data aggregated from simulations. Even though, some circuit optimization methods are proposed, e.g., in [23, 24], the comprehensive method to estimate the initial values for the circuit evaluation has not been provided, according to the best knowledge of authors. Since the single-resonant dipoles are designed to operate at their lowest resonant frequencies, higher-order resonant modes are ignored in equivalents [25].

(a)   (b)
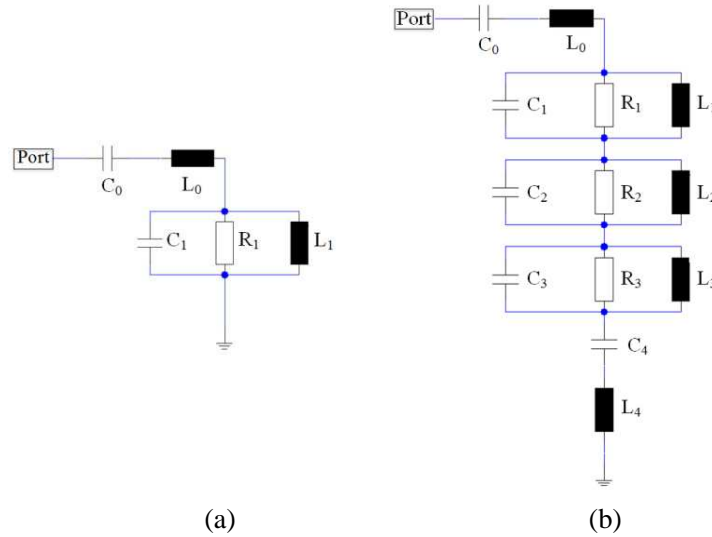
Figure 2. CST simulation models for designed antenna equivalent circuits for planar, (a) single-resonant and (b) multi-resonant UWB dipoles. Each parallel-resonant circuit is to form a resonance.

Based on the antenna impedances acquired from 3D EM-simulations, the determination of the equivalent circuit in Figure 2(a) is started by defining the proper behaviour for input impedance Z_{in}, which is separated for single-resonant circuits according to series and parallel stages as

$$Z_{in} = Z_0 + Z_1. \tag{2}$$

The behaviour of Z_1 for equivalent is formed with the parallel-resonant circuit that includes R_1, L_1 and C_1. First, the initial graph for real impedance is evaluated by fixing either L_1 or C_1 and solving that was left unknown in (1) for the frequency of interest. The magnitude of Z_1 impedance peak can be directly determined by using R_1. After deriving the initial graph for the impedance, it is finally defined by adjusting proper bandwidth with the ratio of L_1/C_1 and fine-tuning resistance with R_1. Fundamentally, C_1 and L_1 which are in parallel with R_1 work as a low-pass filter.

Impedance Z_0 including the series elements C_0 and L_0 forms a high-pass filter is ignored at the beginning respectively with [16], in order to make minor adjustments for the final circuits, since those components are used to adjust impedance to $50\,\Omega$ feed line. The purpose of C_0 and L_0 is to compensate reactive impedance of parallel-resonant circuit in order to maximise the matching.

Since being the combination of high- and low-pass filters, the entire equivalent circuit works fundamentally as a band-pass filter. The equivalence with an UWB antenna is excellent because of antenna's band-pass filter fashion, thus such a circuit topology in Figure 2(b) is feasible for the interest of this study.

In practice, antenna input impedance Z_{in} includes input resistance R_{in} as [26, 27]

$$Z_{in} = R_{in} + jX_{in} = (R_r + R_L) + jX_{in}, \tag{3}$$

where X_{in} is the input reactance, and the content of R_{in} consists of the radiation and loss resistances (R_r, R_L) of the antenna. The influence of R_{in} of the single-resonant dipole on the parallel-resonant degree of equivalent circuit causes the LC resonance to appear lower than can be postulated by using (1). If one considers a lossless antenna, the real part of Z_{in} reduces to R_r as $\mathrm{Re}\{Z_{in}\} = \mathrm{Re}\{R_{in}\} = R_r$ resulting to the radiation of real power as "the power at the antenna input terminals is equated to the power at the current maximum" [26]. The circuit element values for the equivalent circuits of single-resonant UWB dipoles are given on Table 2.

Even though the nature of antenna covering extremely wide bandwidth as the entire FCC UWB band is not the resonant-type, they do practically consist of multiple resonances due to the coverage of bandwidth of 7.5 GHz. In multi-resonant UWB equivalent, each parallel-resonant circuit are used to generate a resonance. Multi-resonant equivalent circuit is determined identically with respect to

Table 2. Element values of equivalent circuits for single-resonant UWB dipoles in Figure 2(a).

Values	3 GHz dipole	6 GHz dipole	9 GHz dipole
C_0	0.41 pF	0.17 pF	0.16 pF
L_0	1.39 nH	1.02 nH	0.001 nH
C_1	0.43 pF	0.17 pF	0.09 pF
L_1	3.38 nH	2.10 nH	1.36 nH
R_1	256.55 Ω	270.26 Ω	348.71 Ω

Table 3. Element values of equivalent circuits for multi-resonant ultra wideband dipole in Figure 2(b).

n	C_n	L_n	R_n
0	1.38 pF	0.39 nH	-
1	0.60 pF	2.03 nH	80.43 Ω
2	0.78 pF	0.33 nH	67.32 Ω
3	0.67 pF	0.19 nH	73.18 Ω
4	1.08 pF	0.34 nH	-

the method presented above. In this case, two additional parallel-resonant degrees Z_2 and Z_3, and a series-resonant circuit Z_4 are added for the introduced resonances as shown in Figure 2(b). As with the single-resonance case, series components (C_0, C_4, L_0 and L_4) are for the adjustment of the impedance to 50 Ω feed line for the final circuit after the proper impedance behaviour with parallel resonant degrees Z_1, Z_2 and Z_3 is determined. The element values on Table 3 are for the multi-resonant UWB antenna equivalent circuit.

3. RESULTS

Equivalent circuits simplify the analysis of dipole impedance significantly, because of enabling to show directly the variation of inductance, capacitance or resistance of an equivalent model for antenna impedance parameters. On the other hand, even though nowadays accurate simulators are relatively fast, the equivalent circuit can show the effect of variation of a circuit parameter on antenna parameters in real time, for which the simulators do not have a capacity. This is because time domain transient takes always time (some minutes or more), depending on the complexity and required mesh properties for the antenna under study. The efficient utilization of equivalents is possible, after the definition of circuit values to characterize the parameters of the antenna of interest properly.

The applicability of the circuits for the accurate modelling of the dipole's impedance parameters is verified by comparing the results with the originally simulated data. The operation is depicted in terms of both reflection coefficient S_{11}, which is defined as

$$S_{11} = (Z_{in} - Z_{TL})/(Z_{in} + Z_{TL}), \tag{4}$$

where Z_{TL} is the impedance of a transmission line, and the real part of Z_{in}. As it is obvious from Figures 3(a)–(b), the defined equivalents can model excellently antenna input impedance Z_{in} as well as antenna reflection coefficient S_{11}, which is probably the most important parameter for antenna engineer. Figure 3(a) further shows that the designed antennas exhibit proper matching for the frequencies of interest.

The physical antenna dimensions were varied during simulations in order to find their impact on antenna impedance parameters. Also equivalent circuit component values were swept to find correspondence between physical antenna dimensions and equivalent models. As a result of this, the operation of a single-resonant dipole and its equivalent is shown in Figure 4(a) in detail.

It is obvious from the demonstration that 1) series-resonant circuit has analogue to the antenna feeding area and mainly defines the antenna matching in terms of S_{11}, and 2) parallel-resonant circuit
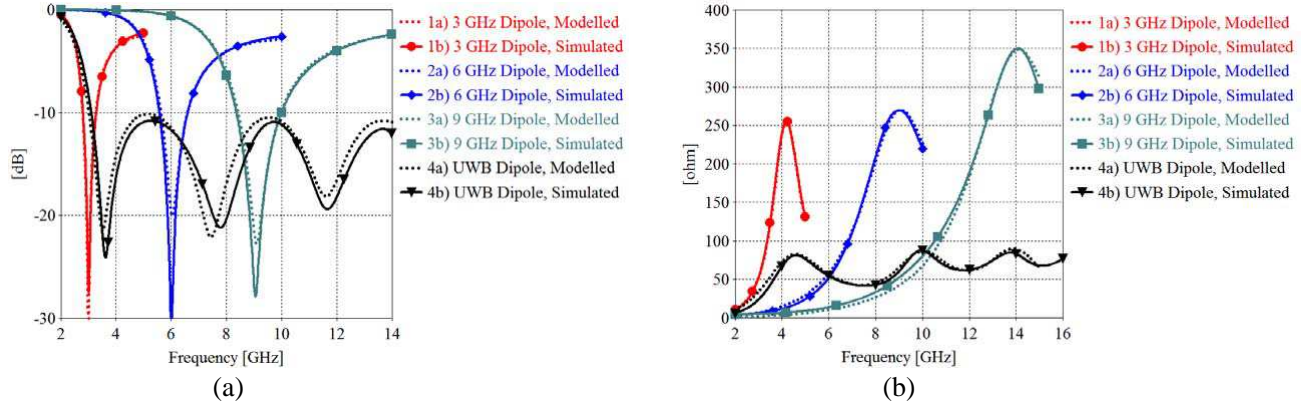
Figure 3. Figure compares (a) reflection coefficient S_{11} [dB] and (b) real input impedance Z_A [ohm] for the simulated single- and multi-resonant UWB dipoles and equivalent circuits.
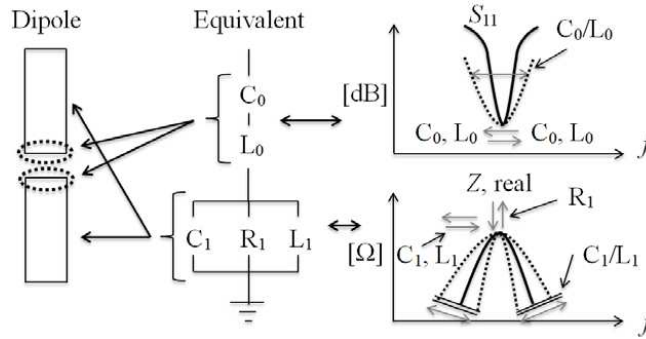
Figure 4. The impedance dependency of dipole and equivalent circuit UWB antenna is depicted.

has equivalence to the practical dipole dimensions as a length and width, and mainly determines the antenna input impedance Z_{in}. In addition to these, the results of this study show that the variation of antenna resonant frequency and matching bandwidth can be separated in these circuit stages, which are discussed in the next subsections in detail.

3.1. Parallel-resonant Circuit

The variation of the size of two symmetrical arms of a single-resonant dipole is observed to correspond with the variation of parallel-resonant stage of equivalent circuit. Parallel resistance R_1 of RLC circuit is seen to show the value for the maximum of the real Z_1, thus it is equal to $R_{in,\max}$. Also the change of value of R_1 has an analogue to variation of the resonant-circle in the Smith Chart in horizontal axis. The variation of R_1 influences on the magnitude of real Z_1, which is shown in Figure 5(a) and compared with the variation of the width of single-resonant dipole.

In theory, the width of an ideal antenna does not have effect on Z_{in} in resonance, although there might be some exceptions as explained in [26]. This can be seen in left Figure 5(a) where R_{in} which is in resonance at 3 GHz does not change. Therefore, to acquire the equal behaviour for the variation of the dipole width and equivalent in right Figure 5(a), the effect of C_1 and L_1 should be taken into account.

Meanwhile R_1 mainly defines the amount of resistance for the resonance peak in (1), the operation frequency in such a cascaded RLC network can be varied with the ratio of C_1 and L_1 if another component is varied while the leftover stays fixed: e.g., the more inductive rate, the lower resonance frequency. Figure 5(b) shows the variation of dipole length and behaviour with an equivalent circuit. The increase of the length is observed to cause increase of L_1, while capacitance remains constant (see values in label). Naturally, R_{in} varies with the length, which absolute value can be directly taken from
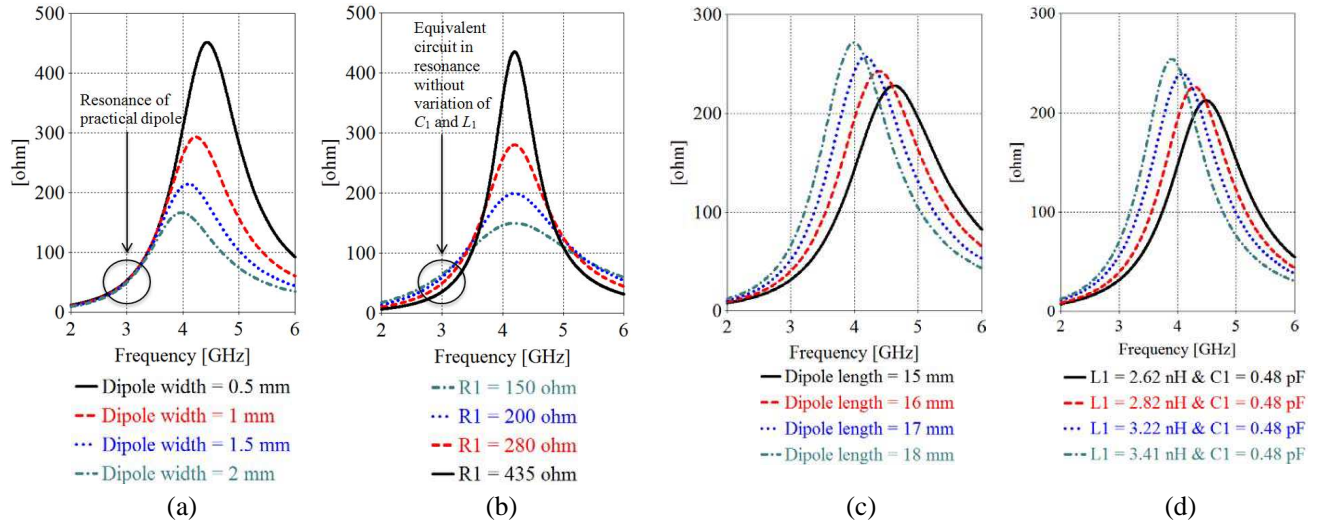
Figure 5. The variation of the (a), (b) width and (c), (d) length of a 3 GHz single-resonant dipole (a), (c) against the variation of parallel-resonant stage equivalent circuit component values.
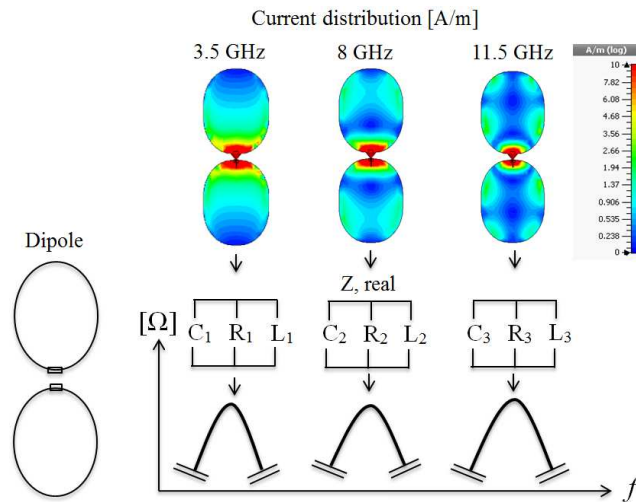
Figure 6. The operation of multi-resonant UWB equivalent circuit. In equivalent, resonances in structure can be defined with an additional parallel-circuit stage. There are multiple current maximum for broadband dipole in higher frequencies.

the impedance peak maximum.

The increase of bandwidth for a dipole means the increase of the antenna width in practice, which has analogue to the addition of capacitance for the circuit. It can be also formulated as the wider the dipole, the slower the variation of input reactance value in (3). That is, because input reactance has a clear connection to the radius a of wire dipole via [18]

$$X_{in} = -120([\ln{(l/2a)} - 1] / \tan{(kl/2)}) \tag{5}$$

[26], where an electrical equivalent planar width w_{planar} can be approximated as $a = 0.25 w_{\mathrm{planar}}$ when the thickness of the radiator is $t_{\mathrm{planar}} \cong 0$ [26, 27].

The operation of multi-resonant UWB dipole is shown in Figure 6. The increase for the width of multi-resonant dipole introduced in Figure 1 has an effect mainly on the decrease of the lowest resonant. However, the changes for the width or length of multi-resonant dipole also influences for the resonances of higher frequencies due to the antenna characteristics to generate resonances. That is because the
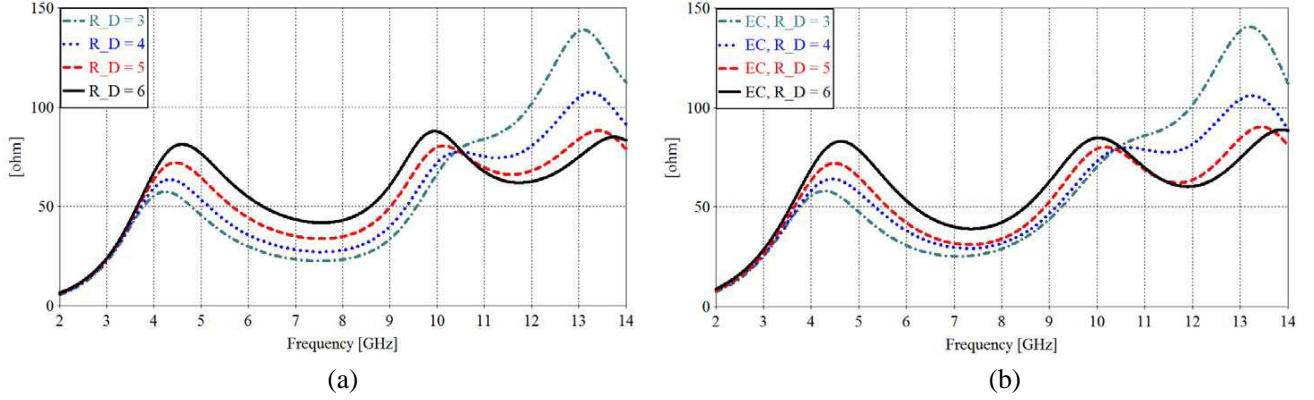
Figure 7. The effect of multi-resonant UWB dipole rounding R_D (R_D) on antenna impedance based on (a) dipole simulation results and (b) corresponging behaviour with the equivalent circuit (EC).

Table 4. Parallel-circuit stage element values of multi-resonant equivalent circuit (EC) for dipole arm rounding modification in Figure 7(b).

component	EC, $R_D = 3$	EC, $R_D = 4$	EC, $R_D = 5$	EC, $R_D = 6$
C_1	1.07 pF	0.88 pF	0.81 pF	0.67 pF
C_2	0.82 pF	0.86 pF	0.88 pF	0.78 pF
C_3	0.46 pF	0.59 pF	0.73 pF	0.67 pF
L_1	1.31 nH	1.46 nH	1.57 nH	1.78 nH
L_2	0.28 nH	0.27 nH	0.28 nH	0.33 nH
L_3	0.31 nH	0.24 nH	0.19 nH	0.19 nH
R_1	55.97 Ω	61.94 Ω	70.00 Ω	80.43 Ω
R_2	55.61 Ω	57.76Ω	63.80Ω	67.32Ω
R_3	118.81 Ω	86.46 Ω	74.57 Ω	73.18 Ω

lowest resonance is generated with the length and the two higher resonances with the shape of antenna.

The variation of the length of UWB dipole means that resonances which are generated by the antenna structure, move up- or downwards. In equivalent, the resonant frequency for structure is performed with the variation of ratio between capacitances C_1, C_2 and C_3 and inductances L_1, L_2 and L_3 in equivalents, also including minor changes for resistances R_1, R_2 and R_3.

The approach of multi-resonant is corresponding with the single-resonant antennas with the exception that for the multi-resonant, dipole arm rounding (i.e., R_D in Figure 1) is required to achieve smooth impedance and matching properties. Figure 7 further demonstrates the effect of variation of R_D for the radius of 3–6 mm for dipole and corresponding behaviour for equivalent. It is obvious from the dipole simulation results that decreasing radius R_D tunes the lowest resonance downwards, while reducing R_{in} and increasing inductance for the lower frequency end. Further, the smaller radius deteriorates the matching of higher UWB band end, as the shape modification increases resistance but also capacitance with smaller inductance's expense. The higher frequencies are more dependent on the rounding of dipole, as visible in current distributions in Figure 6. The variation of multi-resonant equivalent circuit component values is depicted on Table 4. This is the straight benefit of the use of equivalent circuit in analysis: one can see the physical effect based on the increase and decrease of circuit component values.

3.2. Series-Resonant Circuit

During the examinations, the physical dipole feeding (referring to the port connection) area was noticed to have an analogue for the determination of S_{11} of equivalent circuit, which represents how efficiently
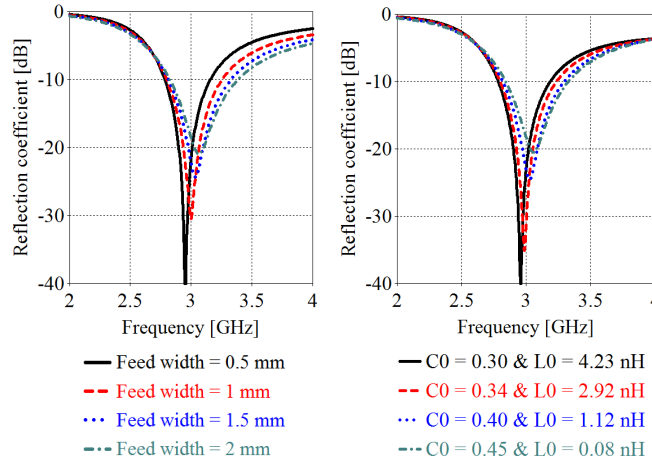
Figure 8. The variation of the feed width for antenna matching.

energy fed in the port is transferred from the port to the structure and resonated in a certain frequency. As the parallel-resonant circuit mainly determines the proper Z_1 behaviour for the structure, S_{11} is adjusted by series-resonant part with components C_0 and L_0. Ratio of C and L components in series-resonant part defines bandwidth for the resonant frequency of S_{11}. This is demonstrated in Figure 8 where the dipole feed width is increased with the proportion of the relative increase of capacitance C_0 of C/L ratio in equivalent series-circuit stage.

Also the gap between the dipole ports (F_D in Figure 1) has influence on impedance: the larger the gap, the higher the resistance, thus narrower the bandwidth and smaller the capacitance.

3.3. The Effect of a Substrate on Antenna Characteristics

Finally, a simple study is carried out in order to demonstrate the effect of a FR4 substrate on antenna performance. The substrate blocks are removed below the copper radiators and 3D EM transients repeated. Then, equivalent circuit models are modified to correspond with the updated antenna structures. The results of evaluation are shown in Figure 9. In addition to depict clearly an absolute shift of the known detuning effect with a substrate, the physical changes in the radiator structures in terms of component values can be conceived with the help of equivalents. The used component values are collected on Table 5. By comparing these values with Tables 2–3, the remarks for the proportion of the effect of a substrate can be stated: the use of a substrate 1) decreases antenna
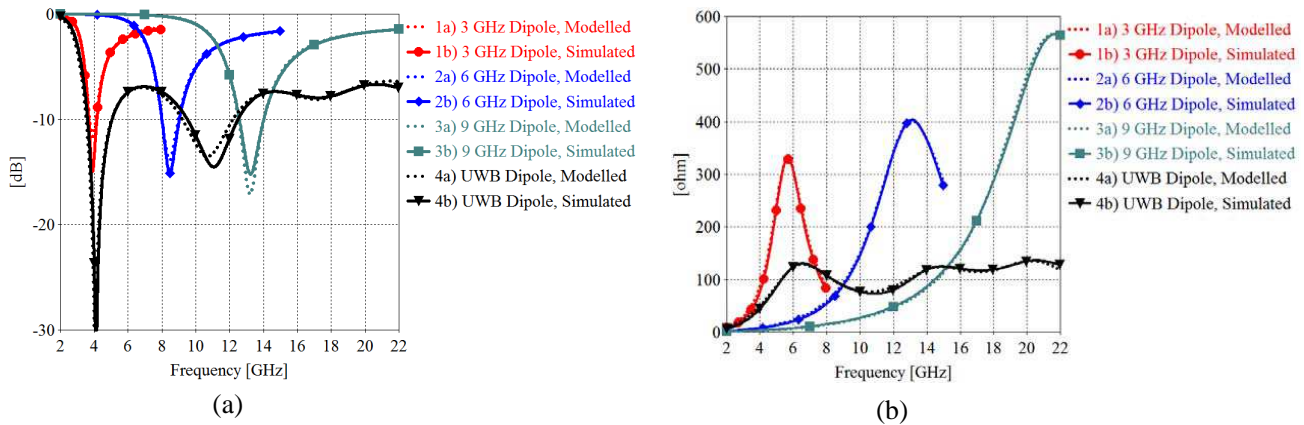
Figure 9. Figure compares (a) reflection coefficient S_{11} [dB] and (b) real input impedance Z_A [ohm] for the simulated single- and multi-resonant UWB dipoles without FR4 substrate below the radiator and equivalent circuits.

Table 5. Element values of equivalent circuits for single- and multi-resonant ultra wideband dipoles in Figure 9(a).

Values	3 GHz dipole	6 GHz dipole	9 GHz dipole
C_0	0.25 pF	0.10 pF	0.06 pF
L_0	0.06 nH	0.43 nH	0.35 nH
C_1	0.20 pF	0.07 pF	0.03 pF
L_1	3.93 nH	2.97 nH	1.55 nH
R_1	330.18 Ω	401.72 Ω	565.95 Ω
	Multi-resonant dipole		
n	C_n	L_n	R_n
0	0.72 pF	0.28 nH	-
1	0.25 pF	2.41 nH	123.28 Ω
2	0.32 pF	0.37 nH	82.07 Ω
3	0.20 pF	0.29 nH	104.61 Ω
4	1.07 pF	0.16 nH	-

resistance significantly, which improves matching of these antennas required to use without matching components and 2) increases relatively capacitance of C/L-ratio, which is the reason to enable slightly wider bandwidth. Even though not being the information of the achieved results but well-known, a substrate further makes possible the implementation of antenna structures to a smaller size.

4. CONCLUSION

In this paper, the impedance dependency of single- and multi-resonant UWB dipoles on antenna dimensions has been examined by using their lumped-element equivalent circuits. The physical antenna dimensions were examined to find both their impact on antenna impedance parameters and correspondence between physical antenna dimensions and equivalent models. The results of this study proved that equivalent circuit can accurately model impedance properties for single- and multi-resonant UWB antennas, also in terms of S_{11}. The series-resonant circuit of equivalent was observed to have analogue to the antenna feeding area and mainly defined the antenna reflection coefficient S_{11}, as it is used to adjust impedance to 50 Ω feed line. Parallel-resonant circuit was noticed to have equivalence to the practical dipole dimensions as a length and width, and mainly determined the antenna input impedance. Moreover, the variation of antenna resonant frequency and impedance bandwidth were observed to be possible to separate in the studied circuit stages. The resistance R_1 of a parallel-resonant circuit in equivalent of a single-resonant antenna has an analogue to the real part of dipole impedance. Also, the resistance has an influence on bandwidth together with the ratio of capacitance C_1 and inductance L_1. Further, the increase of the width of an antenna has an effect on bandwidth, which was concluded to be because of the wider the antenna, the higher the capacitance in the antenna feed. Resonance frequency was determined according to the length of a physical antenna which was equal to the values of C_1 and L_1 in equivalents. Multi-resonant UWB antenna was analysed according to the same principles.

These results extend the knowledge of the impedance dependency of the physical planar UWB dipole antenna dimensions. After understanding the influence of antenna dimensions on impedance, matching can be maximised.

There are several ways in which the content of this study can be extended. The next step is to derive the proportion of body tissues on equivalents and examine UWB antenna operation in the proximity of body tissues. Also the knowledge how a wearable UWB antenna should be designed to mitigate the harmful effects of a body is of interest. Further, the corresponding evaluations for the analysis of wearable textiles with flexible materials are recommended.

REFERENCES

1. "Revision of Part 15 of the Commission's rules regarding ultra wideband transmission systems," FCC Notice of Proposed Rule Making, ET-Docket 98-153, FCC 02-48, 2002.
2. Oppermann, I., M. Hämäläinen, and J. Iinatti, *UWB Theory and Applications,* John Wiley & Sons, England, 2004.
3. Wang, Y., J. Z. Li, and L. X. Ran, "An equivalent circuit modeling method for ultra-wideband antennas," *Progress In Electromagnetics Research*, Vol. 82, 433–445, 2008.
4. Joardar, S. and A. B. Bhattacharya, "A novel method for testing ultra wideband antenna-feeds on radio telescope dish antennas," *Progress In Electromagnetics Research*, Vol. 81, 41–59, 2008.
5. Morton, M. A., J. P. Comeau, J. D. Cressler, M. Michell, and J. Papapolymerou, "Source of phase error and design considerations for silicon-based monolithic high-pass/low-pass microwave phase shifters," *IEEE Trans. Microw. Theory Tech.*, Vol. 54, No. 12, 4032–4040, Dec. 2006.
6. Adamiuk, G., T. Zwick, and W. Wiesbeck, "UWB antennas for communication systems," *Proc. of IEEE*, Vol. 100, No. 7, 2308–2321, Jul. 2012.
7. Jin, X. H., X. D. Huang, C. H. Cheng, and L. Zhu, "Super-wideband printed asymmetrical dipole antenna," *Progress In Electromagnetics Research Letters*, Vol. 27, 117–123, 2011.
8. Chen, Z. N., A. Cai, T. S. P. See, X. Qing, and M. Y. W. Chia, "Small planar UWB antennas in the proximity of the human head," *IEEE Trans. Microw. Theory Tech.*, Vol. 54, No. 4, 146–1857, Apr. 2006.
9. Wiesbeck, W., G. Adamiuk, and C. Sturm, "Basic properties and design principles of UWB antennas," *Proc. of IEEE*, Vol. 97, No. 2, 372–385, Feb. 2009.
10. Tsai, C.-L., "A coplanar-strip dipole antenna for broadband circular polarization operation," *Progress In Electromagnetics Research*, Vol. 121, 141–557, 2011.
11. Klemm, M., I. Z. Kovcs, G. F. Pedersen, and G. Tröster, "Novel small-size directional antenna for UWB WBAN/WPAN applications," *IEEE Trans. Antennas Propag.*, Vol. 53, No. 124, 3884–3896, Dec. 2005.
12. Chahat, N., M. Zhadobov, R. Sauleau, and K. Ito, "A compact UWB antenna for on-body applications," *IEEE Trans. Antennas Propag.*, Vol. 59, No. 4, 1123–1131, Apr. 2011.
13. Ansarizadeh, M. and A. Ghorbani, "An approach to equivalent circuit modeling of rectangular microstrip antennas," *Progress In Electromagnetics Research B*, Vol. 8, 77–86, 2008.
14. Liu, S. F., X. W. Shi, and S. D. Liu, "Study on the impedance-matching technique for high-temperatue superconducting microstrip antennas," *Progress In Electromagnetics Research*, Vol. 77, 281–284, 2007.
15. Akhoondhadeh-Asl, L., M. Fardis, A. Abolghasemi, and G. Dadashzadeh, "Frequency and time domain characteristic of a novel notch frequency UWB antenna," *Progress In Electromagnetics Research*, Vol. 80, 337–348, 2008.
16. Hamid, M. and R. Hamid, "Equivalent circuit of dipole antenna of arbitrary length," *IEEE Trans. Antennas Propag.*, Vol. 45, No. 11, 1695–1696, Nov. 1997.
17. Wang, S. B. T., A. M. Niknejad, and R. W. Brodersen, "Circuit modeling methodology for UWB omnidirectional small antennas," *IEEE J. Sel. Areas Commun.*, Vol. 24, No. 4, 871–877, Apr. 2006.
18. Rambabu, K., M. Ramesh, and A. T. Kalghatgi, "Broadband equivalent circuit of a dipole antenna," *IEE Proceedings — Microwaves, Antennas and Propagation*, Vol. 146, No. 6, 391–393, Dec. 1999.

19. Holopainen, J., R. Valkonen, O. Kivekäs, J. Ilvonen, and P. Vainikainen, "Broadband equivalent circuit model for capacitive coupling element-based mobile terminal antenna," *IEEE Antennas Wireless Propag. Lett.*, Vol. 9, 716–719, 2010.

20. Räisänen, A. V. and A. Lehto, *Radio Engineering for Wireless Communication and Sensor Applications,* Artech House, 2003.

21. Computer Simulation Technology Microwave Studio Software, Online Available: http://www.cst.com.

22. Schelkunoff, S. A., "Theory of antennas of arbitrary size and shape," *Proc. of the IRE*, Vol. 29, 493–521, Sep. 1941.

23. Kim, Y. and H. Ling, "Equivalent circuit modeling of broadband antennas using a rational function approximation," *Microw. and Opt. Tech. Lett.*, Vol. 48, No. 5, 950–953, May 2006.

24. Yarman, B. S., A. Kiling, and A. Aksen, "Immitance data modelling via linear interpolation techniques: A classical circuit theory approach," *Int. J. Circuit Theory Appl.*, Vol. 32, 537–563, 2004.

25. Tang, T. G., Q. M. Tien, and M. W. Gunn, "Equivalent circuit of a dipole antenna using frequency-independent lumped elements," *IEEE Trans. Antennas Propag.*, Vol. 41, No. 1, 100–103, Jan. 1993.

26. Balanis, C. A., *Antenna Theory Analysis and Design,* John Wiley & Sons, 3rd edition, 2005.

27. Stutzman, W. L. and G. A. Thiele, *Antenna Theory and Design,* 2nd edition, John Wiley & Sons, 1998.